

**EXSOLUTION OF ZIRCONIAN-HAFNIAN WODGINITE  
FROM MANGANOAN-TANTALIAN CASSITERITE,  
ANNIE CLAIM #3 GRANITIC PEGMATITE, SOUTHEASTERN MANITOBA, CANADA**

MORGAN MASAU, PETR ČERNÝ<sup>§</sup> AND RON CHAPMAN

*Department of Geological Sciences, University of Manitoba, Winnipeg, Manitoba R3T 2N2, Canada*

ABSTRACT

Primary (Mn,Fe,Ta,Nb)-bearing cassiterite with  $\leq 0.21$  wt.% ZrO<sub>2</sub> and  $\leq 0.05$  wt.% HfO<sub>2</sub> crystallized during the consolidation of the Archean Annie Claim #3 zoned, lepidolite-subtype granitic pegmatite, southeastern Manitoba, in amounts increasing from the outer to the inner pegmatite zones. Rare inclusions of tantalite and ferrotapiolite originated from transient local saturation in these phases. Sparse early cassiterite from the outer intermediate zone is rather rich in substituting elements and in part Fe-dominant, whereas the more abundant late cassiterite from the lepidolite core is strongly Mn-dominant and poor in the substituents. Exsolution in the primary cassiterite generated granular zirconian-hafnian ferrowodginite and wodginite enclosed in veinlets of substituent-depleted cassiterite. The Fe/Mn and Nb/Ta values of the wodginite phases mimic those of the primary cassiterite across the pegmatite zones, and Zr/Hf perceptibly decreases from the outer zones inward. Maximum contents of ZrO<sub>2</sub> and HfO<sub>2</sub> (5.98 and 1.59 wt.%, respectively; 0.31 Zr and 0.04 Hf *apfu*) are the highest so far encountered in wodginite-group minerals. These maxima characterize wodginite exsolved from early cassiterite; the levels drop off in wodginite exsolved in late cassiterite. Instead, hafnian zircon intergrown with abundant thorian coffinite becomes abundant in the lepidolite core, indicating a transition of Zr + Hf from octahedral sites in the oxide minerals to the much more common 8-fold coordination in the orthosilicate; this shift implies a transition from relatively alkaline to more acidic conditions.

*Keywords:* cassiterite, wodginite, ferrowodginite, zirconium, hafnium, granitic pegmatite, Manitoba.

SOMMAIRE

Une cassitérite primaire, enrichie en Mn, Fe, Ta et Nb, et avec  $\leq 0.21\%$  ZrO<sub>2</sub> et  $\leq 0.05\%$  HfO<sub>2</sub> (en poids), a cristallisé au cours de la solidification de la pegmatite granitique archéenne de Annie Claim #3, massif zoné, sous-type à lépidolite, dans le sud-est du Manitoba, en quantités augmentant de la bordure vers le coeur du massif. De rares inclusions de tantalite et de ferrotapiolite ont leur origine dans la saturation temporaire et locale du magma. La cassitérite, assez rare dans la partie externe de la zone intermédiaire, est relativement enrichie en éléments se substituant à l'étain, et elle est en partie à dominance de fer. Par contre, la cassitérite tardive, dans le coeur à lépidolite, est plus abondante, fait preuve d'une dominance de Mn, et est appauvrie dans les autres éléments substituants. L'exsolution a produit des inclusions granulaires de ferrowodginite et de wodginite zirconifère et hafnifère dans des veinules de cassitérite purifiée. Les valeurs Fe/Mn et Nb/Ta des phases du groupe de la wodginite simulent celles de la cassitérite primaire d'une zone à l'autre, et la valeur Zr/Hf diminue de façon subtile de la bordure vers le centre. Les concentrations maximum de ZrO<sub>2</sub> et de HfO<sub>2</sub> (5.98 et 1.59%, respectivement; 0.31 Zr et 0.04 Hf atomes par unité formulaire) sont les plus élevées qui soient connues dans les minéraux du groupe de la wodginite. Ces valeurs élevées caractérisent la wodginite exsolvée de la cassitérite précoce; les taux d'enrichissement diminuent dans la wodginite exsolvée à partir de la cassitérite tardive. En revanche, le zircon hafnifère devient abondant en intercroissance avec la coffinite thoriifère dans la partie centrale à lépidolite, indication d'une transition de Zr + Hf d'une coordination octaédrique dans les oxydes à la coordination huit, beaucoup plus répandue, dans l'orthosilicate. Ce changement impliquerait une transition d'un milieu plutôt alcalin à des conditions davantage acides.

(Traduit par la Rédaction)

*Mots-clés:* cassitérite, wodginite, ferrowodginite, zirconium, hafnium, pegmatite granitique, Manitoba.

<sup>§</sup> E-mail address: p\_cerny@umanitoba.ca

## INTRODUCTION

Cassiterite is well known for its content of mineral inclusions and exsolved phases, both particularly common in high-temperature magmatic parageneses such as those of granitic pegmatites. The most widespread cases are represented by Nb,Ta-oxide minerals, which either predate the crystallization of cassiterite or exsolve from the (Fe, Mn, Ta, Nb)-bearing cassiterite (*e.g.*, Rudakova 1972, Neiva 1996). No other elements, except for minor Ti and W, are known to enter cassiterite in quantities significant enough to control or substantially modify the mineralogy of exsolved phases.

Zirconium and hafnium have only rarely been sought in cassiterite. In the comprehensive study by Möller & Dulski (1983), the levels of these elements were found to be negligible, and on average at a few hundreds and a few tens ppm, respectively. Here, however, we report on cassiterite from a granitic pegmatite that displays a rare dominance of Mn over Fe in its composition, and that contains Zr and Hf in quantities significant enough to generate zirconian-hafnian wodginite by exsolution.

## REGIONAL SETTING AND THE PARENT PEGMATITE

The parent Annie Claim #3 granitic pegmatite is located in the southwestern margin of the Greer Lake pegmatitic granite, intruded in metabasalts of the Lamprey Falls Formation of the Bird River Greenstone Belt, in the Bird River Subprovince of the western part of the Superior province of the Canadian Shield [*cf.* Černý *et al.* (1981) for details of regional geology].

The subellipsoidal, subhorizontal body is approximately 10 × 7 meters in size, with distinct concentric zoning (Masau 1999). The zones show an inward progression of five main types of mica (from muscovite to lithian muscovite and lepidolite), associated mainly with albite and quartz. K-feldspar is subordinate in the outermost zones and missing in the intermediate and inner zones. Accessory minerals include spessartine, cesian beryl, cassiterite, manganocolumbite, manganotantalite and rare primary wodginite, microlite, uranpyrochlore, ferrotapiolite, yttriotantalite or formanite-(Y), apatite, zircon, coffinite, uraninite and xenotime-(Y). The pegmatite and the parent pegmatitic granite do not contain any minerals of B or phosphates of Li, Al, Fe or Mn.

## EXPERIMENTAL

Electron-microprobe analyses of cassiterite and the Ta,Nb-oxide minerals were performed in the wavelength-dispersion mode on a Cameca SX-50 instrument at the Department of Geological Sciences, University of Manitoba. A beam diameter of 1 to 2 μm, accelerating potential of 15 kV, a sample current of 20 nA and a counting time of 20 s were used for Sn in cassiterite (and Ca, Nb, and Ta in the Ta,Nb-oxide minerals), and 40 nA and 50 s for W, Ta, Nb, Fe, Mn, Sb, Bi, As, Zr

and Hf in cassiterite (and Fe, Mn, Pb, Y, Sb, Bi, As, Sn, Zr, Hf, Ti, U and W in the Ta,Nb-oxide minerals). The following standards were used: manganotantalite (TaMα), MnNb<sub>2</sub>O<sub>6</sub> (MnKα, NbLα), FeNb<sub>2</sub>O<sub>6</sub> (FeKα), MgNb<sub>2</sub>O<sub>6</sub> (MgKα), gahnite (ZnKα), CaNb<sub>2</sub>O<sub>6</sub> (CaKα), SnO<sub>2</sub> (SnLα), rutile (TiKα), BiTaO<sub>4</sub> (BiMβ), mimetite (PbMβ, AsLα), stibiotantalite (SbLα), NaScSi<sub>2</sub>O<sub>6</sub> (ScKα), UO<sub>2</sub> (UMβ), ThO<sub>2</sub> (ThMα), YAG (YLα), ZrO<sub>2</sub> (ZrLα), metallic Hf (HfMα) and CaWO<sub>4</sub> (WLα). Data were reduced using the PAP routine of Pouchou & Pichoir (1984, 1985). The lowest contents of U, Th, Pb and some other elements are below the conventional detection-limits, but comparable to the concentrations confirmed by inductively coupled plasma – mass-spectrometer analysis of other minerals under current study. Nevertheless, the quantities given below should be taken as indicative of order of magnitude, rather than at face value.

Identification of wodginite (monoclinic), which is commonly indistinguishable from ixiolite (ideally orthorhombic) by chemical composition, was a daunting task because of the minute grain-size of this phase. A chip ~0.06 mm in size was extracted from a polished thin section, unavoidably contaminated by the host cassiterite, pulverized and X-rayed in a 114.6 mm Debye-Scherrer camera with a Gandolfi attachment for 11 hours, using Ni-filtered CuKα radiation (λ = 1.5406 Å). The identity of wodginite was confirmed by, *i.a.*, comparison with the X-ray diffraction pattern of wodginite G69-23(c), documented as a highly ordered phase by Ercit *et al.* (1992), and examined here under the same conditions as the Annie Claim #3 mineral.

## CASSITERITE AND ASSOCIATED PHASES

Cassiterite occurs in three zones of the pegmatite, associated with greenish muscovite in the outer intermediate zone, with silvery lithian muscovite in the inner intermediate zone, and with purple lepidolite in the core. The abundance of cassiterite increases from rather rare in the outer intermediate zone to fairly widespread in the core. The black grains range from 2 to 15 mm in size. They are usually anhedral, commonly interstitial to divergent blades of albite, cleavelandite habit; subhedral stubby prismatic crystals are found locally in quartz.

In transmitted light, cassiterite shows oscillatory growth-induced zoning, with alternating clear to tan and rusty red or reddish brown to black colors. Growth- and deformation-induced twins are revealed by the study of thin sections.

Textural relations and chemical compositions of the phases within the grains of primary (Ta,Mn)-enriched cassiterite indicate the presence of inclusions of ferrotantalite–manganotantalite and ferrotapiolite, and of exsolved grains of zirconian-hafnian wodginite in a locally (Ta,Mn)-depleted cassiterite matrix. The inclusions seem to be restricted to the dark zones of cassiterite.

ite from the two intermediate zones of the pegmatite. In contrast, exsolution of wodginite is encountered in both dark and pale-colored zones of cassiterite, but is much less important in the latter (Figs. 1, 2). Extremely rare inclusions of formanite or yttrotantalite, and late veining by (Ta,Mn)-depleted cassiterite and microlite also are present but not dealt with in this paper.

#### Primary cassiterite

Cassiterite displays a broad range of fractionation of Mn from Fe. The Fe-dominant compositions are typical of the outer intermediate zone, but most of the samples are distinctly Mn-rich and restricted to the inner intermediate and core zones. In contrast, Ta is consistently more abundant than Nb, and the Ta/(Ta + Nb) value is randomly variable within a narrow range (Fig. 3A; the apparent gap in the distribution of compositions from the outer intermediate zone is probably a sampling artifact, as cassiterite is not particularly abundant in this zone). However, the overall extent of substitution of all

cations for Sn is less than 9 at.% in all cases (Fig. 3B). The highest degree of substitution is observed in cassiterite from the outer intermediate zone (Table 1, composition 6 to 8) and gradually falls off inward (Fig. 4). The average  $ZrO_2$  content is 0.07 wt.% (including values below the formal detection-limits), and the maximum content is 0.21 wt.%; hafnium is in most cases not detectable by electron microprobe. The mechanisms of substitution are not clearly defined, as the contents of some elements are quite low in many cases and, consequently, prone to increased analytical error, but there should not be any doubt about the validity of the simple substitution  $(Ti,Zr,Hf)Sn_{-1}$ , and about the dominant (and possibly exclusive) substitution  $(Mn,Fe)(Ta,Nb)_2Sn_{-3}$ . Cation sums within  $\pm 1\%$  of 1 *apfu* (atom per formula unit) indicate that all the Mn and Fe is divalent.

#### Inclusions of ferrotantalite–manganotantalite

The chemical composition and optical behavior in reflected light leave no doubt about the identity of microscopic Ta-dominant inclusions ( $\leq 20 \mu\text{m}$ ). In the columbite quadrilateral, the compositions are scattered

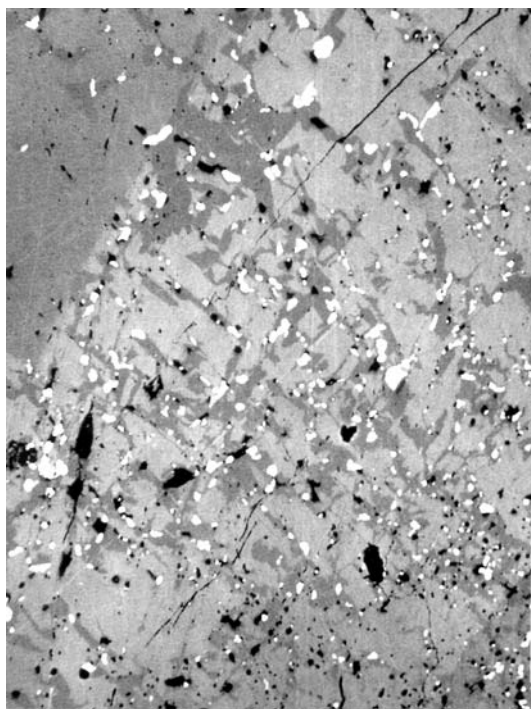


FIG. 1. A BSE image of primary cassiterite (pale grey matrix) criss-crossed by veinlets and patches of depleted cassiterite (darker grey) with exsolution-induced domains of zirconian-hafnian wodginite (white). Note the presence of a (Ta,Nb)-poor zone of cassiterite (dark grey, upper left), in which the exsolution is very restricted. The width of the field of view is 600  $\mu\text{m}$ .

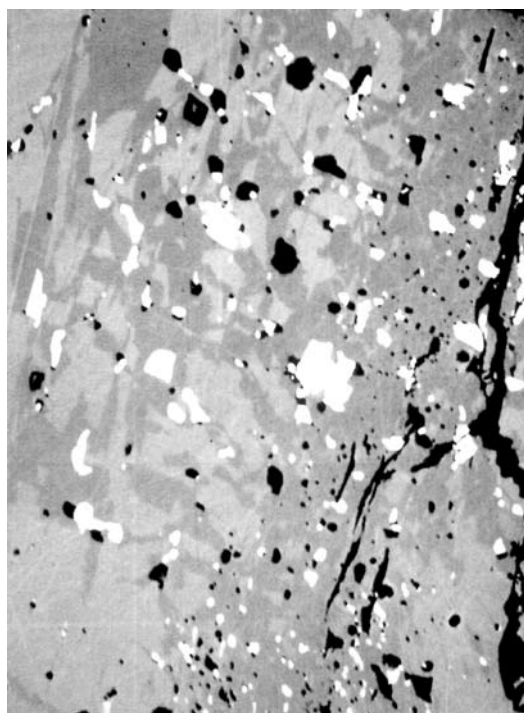


FIG. 2. BSE image of primary cassiterite (pale grey matrix) with a network of depleted cassiterite (dark grey) with exsolved grains of zirconian-hafnian wodginite (white). Note the inverse relationship between the size and number of wodginite grains. The width of the field of view is 220  $\mu\text{m}$ .

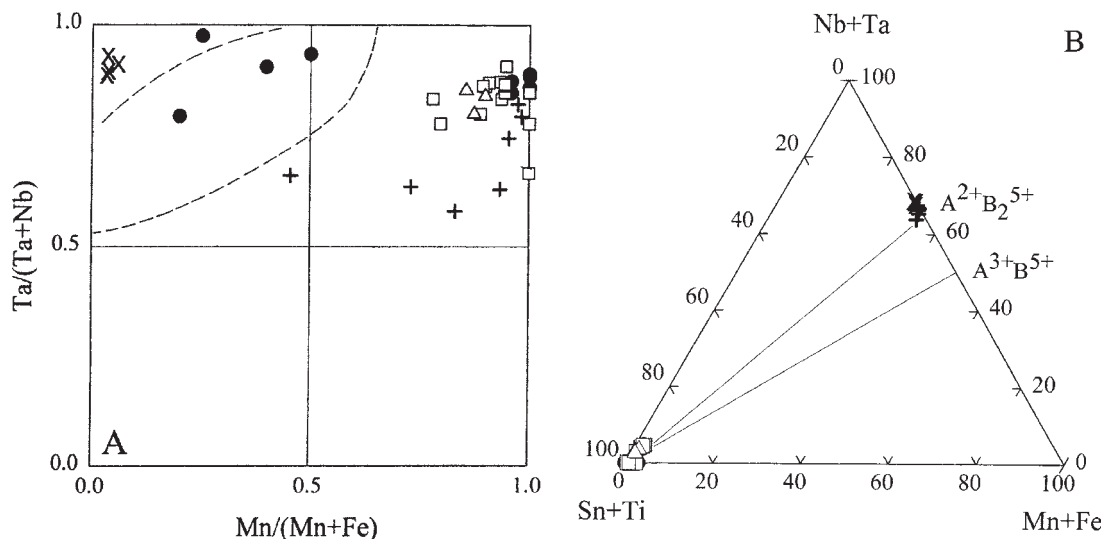


FIG. 3. Compositions of primary cassiterite from the outer intermediate zone (solid circles), inner intermediate zone (open squares) and lepidolite core (open triangles); ferrotantalite – manganotantalite inclusions (crosses), and ferrotapiolite inclusions (x) in the columbite quadrilateral (A) and in the (Ti,Sn) – (Nb,Ta) – (Fe,Mn) diagram (B; both in atomic ratios). In (A), all Fe-dominant data for cassiterite come from the outer intermediate zone, but some compositions from this zone coincide with the Mn-dominant data from the more fractionated inner zones; the two-phase field separating ferrotapiolite from columbite-tantalite is taken from Černý *et al.* (1992). In (B), cassiterite is shown to contain less than 9% of cations substituting for Sn; both tantalite and ferrotapiolite are very poor in tetravalent cations.

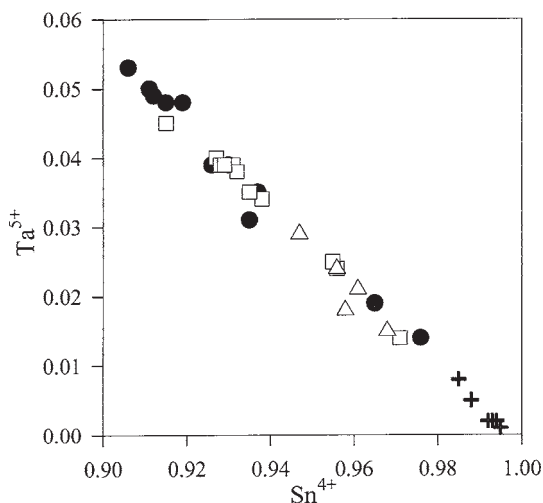


FIG. 4. Inverse correlation of Sn with Ta (both in apfu) in primary cassiterite from the outer (solid dots) and inner (open squares) intermediate zones, and from the lepidolite core (open triangles). Depleted cassiterite (crosses) associated with exsolved wadginite is very Ta-poor.

in an apparently random manner (Fig. 3A). However, the dominance of Ta and Mn in manganotantalite is prevalent; a single Fe-rich composition of ferrotantalite is exceptional. Levels of Ti, W and Zr are very low, and  $Fe^{3+}$  is virtually absent, as shown by the statistically ideal sums of cations and close adherence to the  $(Mn,Fe)(Ta,Nb)_2$  ratio (Table 1, Fig. 3B). The contents of Zr and Hf are low and erratic.

#### Inclusions of ferrotapiolite

The chemical composition of the inclusions of ferrotapiolite ( $\leq 15 \mu m$ ) identifies them beyond reasonable doubt (Table 1). The Fe- and Ta-dominant compositions, tightly clustered in the columbite quadrilateral (Fig. 3A), show only negligible concentrations of cations other than Mn and Nb (Table 1, Fig. 3B). Again, the calculated atomic contents indicate that the presence of an  $A^{3+}B^{5+}O_4$  component is negligible (Table 1, Fig. 3B). The contents of Zr and Hf are very low, at about the detection limit considering the conditions of analysis, and are nonsystematic.

#### Exsolution products: depleted cassiterite and zirconian-hafnian wadginite

In all three zones of the pegmatite, primary cassiterite is invariably criss-crossed by a network of irregular

TABLE 1. REPRESENTATIVE CHEMICAL COMPOSITIONS OF CASSITERITE, INCLUSIONS, AND EXSOLVED WODGINITE AND FERROWODGINITE FROM THE ANNIE CLAIM #3 GRANITIC PEGMATITE, MANITOBA

	inclusions of					primary cassiterite			depleted cassiterite		exsolved wodginite and ferrowodginite			
	manganotantalite			ferrotapiolite		6	7	8	9	10	11	12	13	14
	1	2	3	4	5									
WO <sub>3</sub> wt%	3.52	0.00	0.00	0.08	0.14	0.00	0.00	0.24	0.11	0.01	0.21	0.00	0.00	1.34
Nb <sub>2</sub> O <sub>5</sub>	19.72	14.41	9.80	6.54	2.61	0.53	0.75	0.79	0.00	0.06	7.17	7.33	10.03	7.38
Ta <sub>2</sub> O <sub>5</sub>	57.29	70.10	74.92	78.17	82.52	5.58	7.25	6.51	0.68	0.31	63.11	62.12	58.89	60.27
TiO <sub>2</sub>	0.44	0.08	0.03	0.00	0.23	0.00	0.00	0.00	0.05	0.08	0.14	0.00	0.01	0.02
ZrO <sub>2</sub>	0.00	0.00	0.00	0.00	0.00	0.09	0.12	0.21	0.04	0.00	1.67	2.02	3.91	5.98
HfO <sub>2</sub>	0.00	0.00	0.00	0.00	0.00	0.00	0.00	0.00	0.00	0.00	0.38	0.52	0.77	1.59
SnO <sub>2</sub>	1.32	0.04	0.16	0.44	0.61	92.82	89.64	90.96	99.26	100.10	14.29	15.36	13.08	10.17
ThO <sub>2</sub>	0.00	0.00	0.00	0.13	0.00	0.00	0.06	0.00	0.00	0.01	0.00	0.00	0.00	0.13
UO <sub>2</sub>	0.00	0.13	0.00	0.00	0.02	0.00	0.00	0.00	0.00	0.00	0.11	0.00	0.01	0.08
Sc <sub>2</sub> O <sub>3</sub>	0.42	0.00	0.00	0.01	0.00	0.00	0.00	0.00	0.00	0.00	0.00	0.00	0.00	0.00
Fe <sub>2</sub> O <sub>3</sub>	0.13	0.00	0.00	0.00	0.00	0.00	0.00	0.00	0.00	0.00	0.00	0.00	1.00	0.00
As <sub>2</sub> O <sub>3</sub>	0.00	0.02	0.04	0.05	0.02	0.01	0.03	0.03	0.00	0.04	0.03	0.07	0.04	0.08
Y <sub>2</sub> O <sub>3</sub>	0.00	0.00	0.00	0.00	0.00	0.00	0.01	0.00	0.00	0.01	0.00	0.00	0.00	0.00
Sb <sub>2</sub> O <sub>3</sub>	0.01	0.00	0.00	0.00	0.00	0.07	0.03	0.07	0.04	0.05	0.02	0.01	0.00	0.00
Bi <sub>2</sub> O <sub>3</sub>	0.00	0.00	0.00	0.00	0.07	0.00	0.04	0.00	0.00	0.01	0.00	0.00	0.00	0.00
MgO	0.01	0.01	0.00	0.00	0.00	0.00	0.00	0.00	0.02	0.00	0.00	0.00	0.03	0.01
CaO	0.00	0.00	0.04	0.01	0.00	0.05	0.05	0.03	0.04	0.05	0.01	0.00	0.04	0.01
MnO	11.26	14.16	14.14	0.45	0.57	0.80	1.13	0.85	0.12	0.00	10.83	10.85	3.85	6.24
FeO	4.03	0.68	0.37	13.27	12.83	0.08	0.03	0.22	0.01	0.03	1.16	0.86	7.78	5.68
ZnO	0.00	0.00	0.00	0.00	0.07	0.00	0.00	0.00	0.00	0.00	0.00	0.00	0.00	0.07
PbO	0.00	0.00	0.03	0.09	0.09	0.02	0.00	0.00	0.09	0.03	0.20	0.00	0.11	0.00
Total	98.15	99.63	99.53	99.24	99.78	100.14	99.14	99.91	100.52	100.82	99.33	99.14	99.55	99.05
atomic contents*														
W <i>apfu</i>	0.276	0.000	0.000	0.002	0.003	0.000	0.000	0.002	0.001	0.000	0.006	0.000	0.000	0.037
Nb	2.698	2.037	1.426	0.244	0.099	0.006	0.009	0.009	0.000	0.001	0.346	0.353	0.470	0.353
Ta	4.714	5.961	6.558	1.757	1.887	0.038	0.050	0.045	0.005	0.002	1.833	1.802	1.661	1.736
Ti	0.100	0.019	0.007	0.000	0.015	0.000	0.000	0.000	0.001	0.001	0.011	0.000	0.001	0.002
Zr	0.000	0.000	0.000	0.000	0.000	0.001	0.001	0.003	0.000	0.000	0.087	0.105	0.198	0.309
Hf	0.000	0.000	0.000	0.000	0.000	0.000	0.000	0.000	0.000	0.000	0.012	0.016	0.023	0.048
Sn	1.159	0.005	0.021	0.015	0.020	0.932	0.911	0.915	0.988	0.993	0.608	0.653	0.541	0.430
Th	0.000	0.000	0.000	0.002	0.000	0.000	0.000	0.000	0.000	0.000	0.000	0.000	0.000	0.003
U	0.000	0.009	0.000	0.000	0.000	0.000	0.000	0.000	0.000	0.000	0.003	0.000	0.000	0.002
Sc	0.111	0.000	0.000	0.001	0.000	0.000	0.000	0.000	0.000	0.000	0.000	0.000	0.000	0.000
Fe <sup>3+</sup>	0.029	0.000	0.000	0.000	0.000	0.000	0.000	0.000	0.000	0.000	0.000	0.000	0.078	0.000
As	0.000	0.004	0.008	0.003	0.001	0.000	0.000	0.000	0.000	0.001	0.002	0.005	0.003	0.005
Sb	0.001	0.000	0.000	0.000	0.000	0.001	0.000	0.001	0.000	0.001	0.001	0.000	0.000	0.000
Bi	0.000	0.000	0.000	0.000	0.002	0.000	0.000	0.000	0.000	0.000	0.000	0.000	0.000	0.000
Mg	0.005	0.005	0.000	0.000	0.000	0.000	0.000	0.000	0.001	0.000	0.000	0.000	0.005	0.002
Ca	0.000	0.000	0.014	0.001	0.000	0.001	0.001	0.001	0.001	0.001	0.001	0.000	0.004	0.001
Mn	2.886	3.750	3.855	0.032	0.041	0.017	0.024	0.018	0.003	0.000	0.980	0.980	0.338	0.560
Fe <sup>2+</sup>	1.021	0.178	0.100	0.917	0.902	0.002	0.001	0.005	0.000	0.001	0.104	0.077	0.675	0.503
Zn	0.000	0.000	0.000	0.000	0.004	0.000	0.000	0.000	0.000	0.000	0.000	0.000	0.000	0.005
Pb	0.000	0.000	0.003	0.002	0.002	0.000	0.000	0.000	0.001	0.000	0.006	0.000	0.003	0.000
Catsum	12.000	11.968	11.991	2.975	2.977	0.999	0.999	0.998	1.001	1.001	3.998	3.991	4.000	3.996

\* Based on 24 atoms of oxygen and 12 cations for manganotantalite, 6 atoms of oxygen and 3 cations for ferrotapiolite, 2 atoms of oxygen and 1 cation for cassiterite, and 8 atoms of oxygen and 4 cations for wodginite; 0.00 wt.% and 0.000 atoms per formula unit (*apfu*): below detection limit.

veinlets and blebs strongly depleted in all cations substituting for Sn; this network hosts numerous irregular grains of zirconian-hafnian wodginite. The maximum width of the veinlets is about 100  $\mu\text{m}$ , and the size of the wodginite grains attains locally 50  $\mu\text{m}$  but averages  $\sim$ 10  $\mu\text{m}$ . The orientation of the depleted veinlets seems

to be controlled by the crystal structure of the primary cassiterite.

The depleted cassiterite is closer to pure SnO<sub>2</sub> in composition than the primary cassiterite. The levels of Mn, Ta, Fe and Nb are greatly reduced (Fig. 4), and the contents of Zr and Hf are largely below the limits of detection (Table 1).

In contrast, the exsolved wodginite is remarkably enriched not only in Mn, Fe, Ta and Nb, but also in Zr and Hf (Table 1). As with the primary cassiterite discussed above, the Mn/(Mn + Fe) value of wodginite from the outer intermediate zone of the pegmatite is variable. The compositions of some grains from this zone correspond to ferrowodginite, but those from the inner zones of the pegmatite are close to the end-member wodginite *sensu stricto* (Fig. 5A). All compositions, however, show Ta dominant over Nb. The stoichiometry of wodginite is relatively constant, and it is shifted from that of the ideal formula to compositions with slightly lower contents of tetravalent cations and higher proportions of (Ta,Nb) and (Mn,Fe)<sup>2+</sup> (Fig. 5B), with only negligible Fe<sup>3+</sup><sub>calc.</sub> in a few grains.

The maximum values of ZrO<sub>2</sub> and HfO<sub>2</sub> in the exsolved grains of wodginite are 5.98 and 1.59 wt.% (0.309 and 0.048 *apfu* Zr and Hf, respectively). Figure 6 shows that Zr/Hf is generally low, decreasing from the outer intermediate zone (average 3.17) through the inner intermediate zone (2.77) to the lepidolite core (2.61). Absolute concentrations of Zr + Hf decrease in the same direction (Fig. 7).

The Gandolfi X-ray-diffraction pattern of the exsolved Fe-poor wodginite contains diffraction maxima of admixed cassiterite, and the number and absolute intensity of the diffraction maxima of wodginite are reduced. However, the characteristic strong doublet of 221 and 221 is well defined, and yielded  $\Delta 2\theta$  (221 – 221) of 0.46°. Compared to the

wodginite-group databank of Ercit *et al.* (1992), this value corresponds to an interaxial angle  $\beta$  of ~91.1°, which characterizes this wodginite as apparently completely ordered (*cf.* Tables 7 and 8, Fig. 8 in Ercit *et al.* 1992). However, it must be kept in mind that the effect of incorporating Zr<sup>4+</sup> and Hf<sup>4+</sup> into the B site of wodginite structure on the  $\beta$  angle is not known, and the proportion of these cations in the ferrowodginite-wodginite grains examined here is substantial. This is clearly demonstrated by the cation contents of ferrowodginite and wodginite listed in Table 1 (#13 and 14, respectively), which lead to the following formulas (on the assumption of full order among cations): ferrowodginite (Fe<sup>2+</sup><sub>0.650</sub>Mn<sub>0.338</sub>Mg<sub>0.005</sub>Ca<sub>0.004</sub>Pb<sub>0.003</sub>) $\Sigma$ 1.000 (Sn<sub>0.541</sub>Zr<sub>0.198</sub>Hf<sub>0.023</sub>Ta<sub>0.131</sub>Fe<sup>3+</sup><sub>0.078</sub>Fe<sup>2+</sup><sub>0.025</sub>As<sub>0.003</sub>Ti<sub>0.001</sub>) $\Sigma$ 1.000 (Ta<sub>1.530</sub>Nb<sub>0.470</sub>) $\Sigma$ 2.000 O<sub>8</sub>, wodginite (Mn<sub>0.560</sub>Fe<sub>0.432</sub>Zn<sub>0.005</sub>Mg<sub>0.002</sub>Ca<sub>0.001</sub>) $\Sigma$ 1.000 (Sn<sub>0.430</sub>Zr<sub>0.309</sub>Hf<sub>0.048</sub>Ta<sub>0.126</sub>Fe<sup>2+</sup><sub>0.071</sub>As<sub>0.005</sub>Th<sub>0.003</sub>Ti<sub>0.002</sub>U<sub>0.002</sub>) $\Sigma$ 0.996 (Ta<sub>1.610</sub>Nb<sub>0.353</sub>W<sub>0.037</sub>) $\Sigma$ 2.000 O<sub>8</sub>.

## DISCUSSION

### Crystal chemistry of cassiterite

Cassiterite, ideally SnO<sub>2</sub>, usually displays only a limited number of cation substituents, most commonly Fe, Nb, Ta and minor Mn and W (*e.g.*, Clark *et al.* 1976, Foord 1982, Černý & Ercit 1989, Neiva 1996). However, the style of accommodation of the substituting elements and their state are apparently rather complicated.

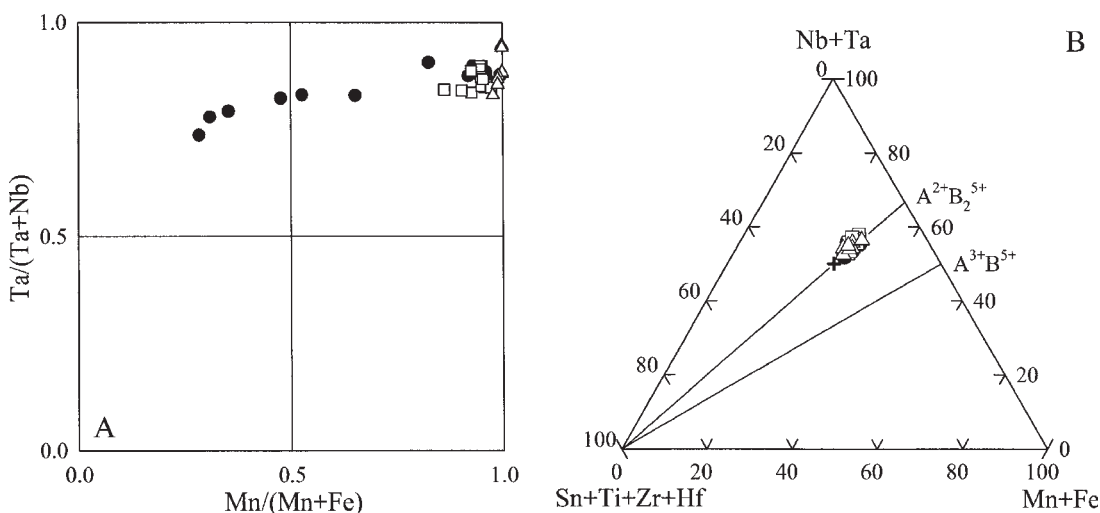


FIG. 5. Compositions of exsolved zirconian-hafnian wodginite in cassiterite of the outer intermediate zone (solid circles), inner intermediate zone (open squares) and lepidolite core (open triangles) in the columbite quadrilateral (A) and in the (Sn, Ti, Zr, Hf) – (Nb, Ta) – (Mn, Fe) diagram (B; both in atomic ratios). In (A), note the similarity with the compositional spread of primary cassiterite in Figure 3A: Fe-dominant compositions are restricted to the outer intermediate zone, but extend into the Mn-dominant part of the diagram, with overlap on the data from the inner zones. In (B), the data cluster very tightly on the (Nb + Ta)- and (Fe + Mn)-enriched side of the ideal stoichiometry of wodginite (cross).

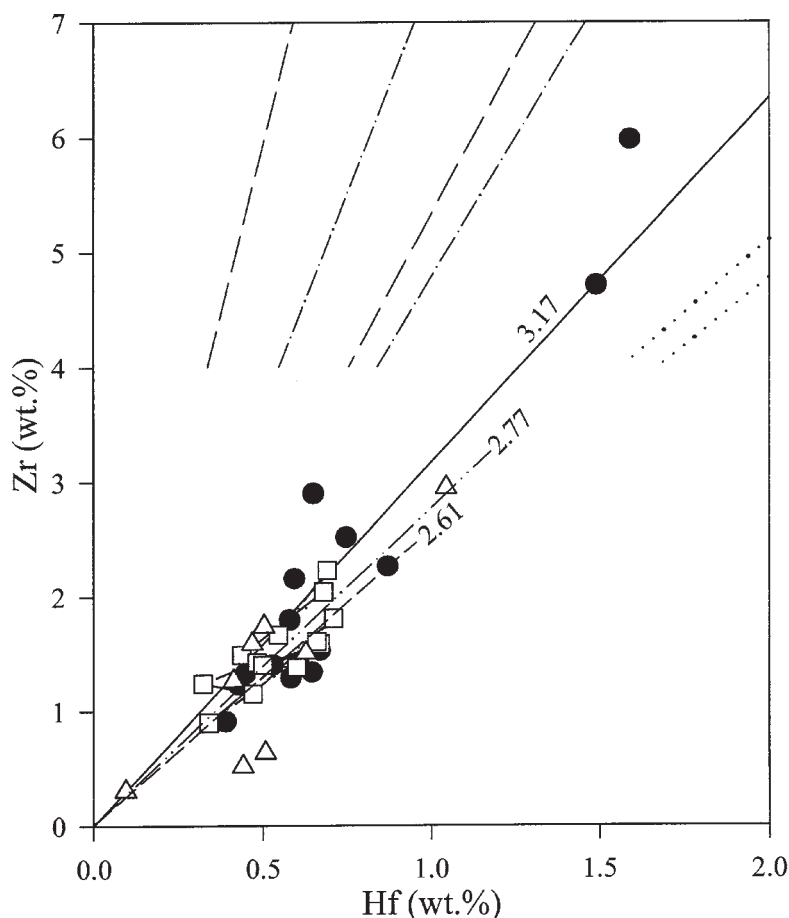


FIG. 6. Concentrations of zirconium *versus* hafnium in exsolved wodginite from the outer intermediate zone (solid circles), inner intermediate zone (open squares) and lepidolite core (open triangles); the regression lines correspond to Zr/Hf of 3.17 (solid line), 2.77 (dash-dot-dot) and 2.61 (short dashes), respectively. Note the maximum enrichment in Zr and Hf in the wodginite from cassiterite of the outer intermediate zone. Locality- and species-dependent regression lines for columbite-tantalite (long dashes), ixiolite (dash-dot) and wodginite (dotted) (Cerný *et al.* 1999) are shown for comparison.

The ratio of  $\text{Fe}^{2+}$  to  $\text{Fe}^{3+}$  is variable, particularly in subsolidus assemblages; incorporation of Fe in the form of stannates and hydroxystannates of iron is claimed by some authors; interstitial  $\text{Sn}^{2+}$  compensated by octahedrally coordinated  $\text{Al}^{3+}$  and  $\text{Fe}^{3+}$  is documented by others, and micro-inclusions of columbite-tantalite or ferrotapiolite are occasionally blamed for the presence of most, if not all, of the Fe, Mn, Ta and Nb (as reviewed by Černý & Ercit 1989, Groat *et al.* 1994). Additional complexities were proposed by Möller *et al.* (1988; tetravalent Nb and Ta?), and Ruck *et al.* (1989;  $\text{Fe}^{3+}\text{OH}$  substituting for  $\text{Sn}^{4+}\text{O}^{2-}$ ). Nevertheless, the maximum concentrations of the major substituents, Fe and Ta + Nb, may attain appreciable levels, which result in the so-called "staringite" (Groat *et al.* 1994).

Zirconium and hafnium are known to substitute for Sn in cassiterite but generally in only trace amounts. Möller & Dulski (1983) reported on Zr and Hf contents of 126 samples of cassiterite from diverse environments: they found maxima of 5200 ppm Zr and 420 ppm Hf, and values exceeding 1000 ppm Zr and 200 ppm Hf in only seven and five samples, respectively.

The primary cassiterite from the Annie Claim #3 pegmatite shows moderate contents of divalent and pentavalent cationic substituents, but it displays a strong dominance of Mn over Fe in most samples. This is in striking contrast to the usual  $\text{Mn}/(\text{Mn} + \text{Fe})$  value, much less than 0.5 (*cf.* Rudakova 1972, Neiva 1996), but in general agreement with extreme fractionation of Mn from Fe, typical for other minerals of the lepidolite-sub-

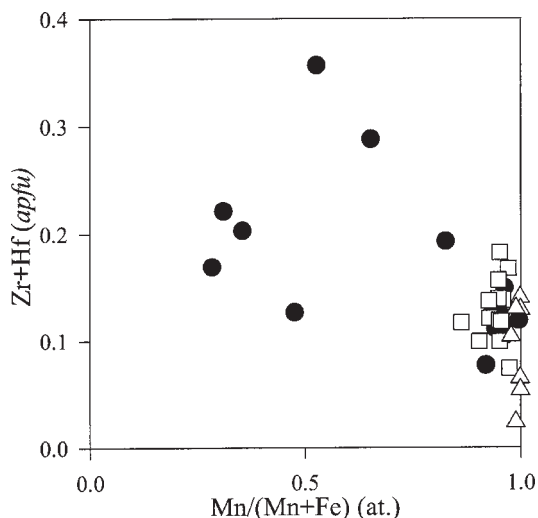


FIG. 7. Inverse correlation of Zr + Hf (apfu) with Mn/(Mn + Fe) (at.) in exsolved ferrowodginite and wodginite from the outer (solid dots) and inner (open squares) intermediate zones, and from the lepidolite core (open triangles).

type pegmatites (*cf.* columbite–tantanalite: Černý & Ercit 1985, Černý & Němec 1995, Masau 1999; lepidolite: Černý *et al.* 1995; garnet: Novák & Povondra 1995). The contents of Zr and Hf are not exceptional, but they fall within the uppermost part of the ranges determined by Möller & Dulski (1983). The contents of Mn, Fe, Ta and Nb, and of both Zr and Hf, decrease during the crystallization of the pegmatite (Fig. 4), and Fe/Mn also decreases in this direction (Fig. 3A).

#### Characteristics of the inclusions

The inclusions of tantalite and ferrotapiolite are rare, distributed in a random manner, and apparently independently of each other. Their compositions are not related to the boundaries of the empirically established miscibility-gap in the columbite quadrilateral, except a single composition of ferrotantalite that is not matched by a ferrotapiolite counterpart (Fig. 3A; see Černý *et al.* 1992). These two species seem to have nucleated owing to rare spots of local saturation prior to or during the growth of the enclosing cassiterite.

#### Exsolution of zirconian-hafnian wodginite

Textural patterns (Fig. 1, 2) and the compositional and volumetric interrelations of depleted cassiterite and wodginite grains (Table 1, Figs. 3, 5) all indicate that these minerals were generated by exsolution from the primary cassiterite. Given suitable low-P–T conditions and probably an action of late pegmatite-related fluids, the structure of cassiterite is evidently not tolerant of

even negligible amounts of Zr and Hf, and these two elements tend to exsolve into a separate (Fe,Mn,Ta,Nb)-rich phase. Both  $Zr^{4+}$  and  $Hf^{4+}$  have a slightly larger  $r_i$  in octahedral coordination than  $Sn^{4+}$  [0.72 and 0.71 versus 0.69 Å: Shannon (1976)], and much more ionic bonds with oxygen [~67 and ~70 versus ~47%: Pauling (1960) in Bloss (1971)].

Attempts at quantitative calculations of the volume proportions of depleted cassiterite and exsolved wodginite relative to the chemical composition of these phases and that of the primary cassiterite proved futile; the Zr plus Hf contents of primary cassiterite, and the Zr, Hf, Nb and Ta contents of depleted cassiterite were in many cases below their detection limits, the composition of wodginite was found to be highly variable among grains within a single low-magnification back-scattered electron (BSE) image, and the inclusions of tantalite and tapiolite were visually difficult to distinguish from those of wodginite. Nevertheless, image analysis adjusted for primary inclusions and modal estimates indicate that the exsolved wodginite constitutes between 10 and 20 vol.% of the veins of depleted cassiterite. The loss of Ta, Nb, Fe and Mn from primary cassiterite amounts to ~80 to 90 at.%, the exsolved wodginite contains about 10 times as much (Mn,Fe) + (Ta,Nb) as the primary cassiterite, and about 20 to 25 times as much (Zr,Hf). All these data, approximations as they largely are, support an exsolution origin of wodginite, if one considers that the structures of both minerals involved are based on chains of corner-sharing octahedra and have near-identical cation contents per unit of volume. Introduction or exchange of cations to the oxide-mineral assemblage during the breakdown must have been minimal, if any.

The exsolution of wodginite-group minerals from cassiterite reminds us of the behavior of Zr and Hf in orthorhombic phases of the columbite group (Černý *et al.* 1998, 1999): columbite–tantanalite contains only modest concentrations of Zr and Hf, but coprecipitated or exsolved ixiolite was shown to accommodate up to 9.55 wt.%  $ZrO_2$  and 1.44 wt.%  $HfO_2$ . Primary wodginite was found to have lower maximal concentrations of these oxides (2.13 and 0.71 wt.%, respectively), but to have the lowest Zr/Hf value (Černý *et al.* 1998, 1999). Thus, the Zr and Hf contents of the exsolved Annie Claim #3 ferrowodginite and wodginite are the highest so far encountered in wodginite-group minerals; the combined maximum contents of Zr + Hf constitute 36% of the B site in the wodginite formula  $ABC_2O_8$ .

#### Summary of the process

Primary cassiterite, with modest contents of Mn, Fe, Ta, Nb and minor Zr and Hf, crystallized during the consolidation of the Annie Claim #3 granitic pegmatite in amounts increasing from the outer to the inner pegmatite zones. Precipitation of rare inclusions of tantalite and ferrotapiolite was triggered by local and



transient saturation in these phases. Rare early cassiterite in the outer intermediate zone is relatively rich in the substituents and is in part Fe-dominant, whereas the more abundant late cassiterite in the lepidolite core is Mn-dominant and relatively poor in the substituting elements. Exsolution in the primary cassiterite generated granular zirconian-hafnian ferrowodginite and wodginite in veinlets of (Mn,Fe,Ta,Nb,Zr,Hf)-depleted cassiterite. The Fe/Mn and Nb/Ta values of the wodginite phases mimic those of the primary cassiterite across the different pegmatite zones, and Zr/Hf decreases slightly from the outer intermediate zone inward. Maximum contents of ZrO<sub>2</sub> and HfO<sub>2</sub> are encountered in wodginite exsolved from the early generation of cassiterite, and they drop off in wodginite blebs in late cassiterite of the lepidolite core. Hafnian zircon intergrown with thorium coffinite is a characteristic constituent of the lepidolite core but is very rare in intermediate zones of the pegmatite (Masau 1999). This distribution of Zr and Hf suggests somewhat more alkaline conditions during most of the pegmatite's consolidation (octahedral coordination of Zr and Hf in oxide phases; cf. Farges *et al.* 1991, 1994, London 1990, 1992), but a transition to a more acidic environment in the lepidolite core (and to the much more common 8-fold coordination in zircon).

## ACKNOWLEDGEMENTS

This work was in part excerpted and upgraded from the B.Sc. Honours thesis of MM, supported by NSERC Major Installation, Equipment and Research Grants to P.C. and Equipment and Infrastructure Grants to F.C. Hawthorne. Mark Cooper kindly confirmed the identity of wodginite by X-ray diffraction. Reviews by T.S. Ercit and A.M.R. Neiva, and the editorial advice of R.F. Martin, are gratefully acknowledged.

## REFERENCES

- BLOSS, F.D. (1971): *Crystallography and Crystal Chemistry*. Holt, Rinehart & Winston, New York, N.Y.
- ČERNÝ, P. & ERCIT, T.S. (1985): Some recent advances in the mineralogy and geochemistry of Nb and Ta in rare-element granitic pegmatites. *Bull. Minéral.* **108**, 499-532.
- \_\_\_\_\_, & \_\_\_\_\_ (1989): Mineralogy of niobium and tantalum: crystal chemical relationships, paragenetic aspects and their economic implications. In *Lanthanides, Tantalum and Niobium* (P. Möller, P. Černý & F. Saupé, eds.). Springer-Verlag, Berlin, Germany (27-79).
- \_\_\_\_\_, \_\_\_\_\_, SMEDS, S.-A., GROAT, L.A. & CHAPMAN, R. (1998): Zirconium and hafnium in minerals of the columbite family. *Geol. Assoc. Can. – Mineral. Assoc. Can., Program Abstr.* **23**, A29-A30.
- \_\_\_\_\_, \_\_\_\_\_, \_\_\_\_\_, \_\_\_\_\_ & \_\_\_\_\_ (1999): Zirconium and hafnium in minerals of the columbite family. *MinWien Conference Vienna, Austria. Ber. Deutsch. Mineral. Ges.* **1**, 47 (abstr.).
- \_\_\_\_\_, \_\_\_\_\_ & WISE, M.A. (1992): The tantalite – tapiolite gap: natural assemblages versus experimental data. *Can. Mineral.* **30**, 587-596.
- \_\_\_\_\_, & NĚMEC, D. (1995): Pristine vs contaminated trends in Nb,Ta-oxide minerals of the Jihlava pegmatite district, Czech Republic. *Mineral. Petrol.* **55**, 117-129.
- \_\_\_\_\_, STANĚK, J., NOVÁK, M., BAADSGAARD, H., RIEDER, M., OTTOLINI, L., KAVALOVÁ, M. & CHAPMAN, R. (1995): Geochemical and structural evolution of micas in the Rožná and Dobrá Voda pegmatites, Czech Republic. *Mineral. Petrol.* **55**, 177-201.
- \_\_\_\_\_, TRUEMAN, D.L., ZIEHLKE, D.V., GOAD, B.E. & PAUL, B.J. (1981): The Cat Lake – Winnipeg River and the Wekusko Lake pegmatite fields, Manitoba. *Manitoba Dep. Energy and Mines, Mineral Res. Div., Econ. Geol. Rep.* **ER80-1**.
- CLARK, A.M., FEJER, E.E., DONALDSON, D.J. & SILVER, J. (1976): The <sup>119</sup>Sn Mossbauer spectra, cell dimensions, and minor element contents of some cassiterites. *Mineral. Mag.* **40**, 895-898.
- ERCIT, T.S., ČERNÝ, P., HAWTHORNE, F.C. & MCCAMMON, C.A. (1992): The wodginite group. II. Crystal chemistry. *Can. Mineral.* **30**, 613-631.
- FARGES, F., BROWN, G.E., JR. & VELDE, D. (1994): Structural environment of Zr in two inosilicates from Cameroon: mineralogical and geochemical implications. *Am. Mineral.* **79**, 838-847.
- \_\_\_\_\_, PONADER, C.W. & BROWN, G.E., JR. (1991): Structural environments of incompatible elements in silicate glass/melt systems. I. Zirconium at trace levels. *Geochim. Cosmochim. Acta* **55**, 1563-1574.
- FOORD, E.E. (1982): Minerals of tin, titanium, niobium and tantalum in granitic pegmatites. In *Granitic Pegmatites in Research and Industry* (P. Černý, ed.). *Mineral. Assoc. Can., Short Course Handbook* **8**, 187-238.
- GROAT, L.A., PUTNIS, A., KISSIN, S.A., ERCIT, T.S., HAWTHORNE, F.C. & GAINES, R.V. (1994): Staringite discredited. *Mineral. Mag.* **58**, 271-277.
- LONDON, D. (1990): Internal differentiation of rare-element pegmatites: a synthesis of recent research. In *Ore-Bearing Granite Systems, Petrogenesis and Mineralizing Processes* (H.J. Stein & J.L. Hannah, eds.). *Geol. Soc. Am., Spec. Pap.* **246**, 35-50.
- \_\_\_\_\_, (1992): The application of experimental petrology to the genesis and crystallization of granitic pegmatites. *Can. Mineral.* **30**, 499-540.
- MASAU, M. (1999): *Mineralogy and Geochemistry of the Annie Claim No. 3 Pegmatite Pod at Greer Lake, Southeastern Manitoba*. B.Sc. thesis, University of Manitoba, Winnipeg, Manitoba.

- MÖLLER, P. & DULSKI, P. (1983): Fractionation of Zr and Hf in cassiterite. *Chem. Geol.* **40**, 1-12.
- \_\_\_\_\_, \_\_\_\_\_, SZACKI, W., MALOW, G. & RIEDEL, E. (1988): Substitution of tin in cassiterite by tantalum, niobium, tungsten, iron, and manganese. *Geochim. Cosmochim. Acta* **52**, 1497-1503.
- NEIVA, A.M.R. (1996): Geochemistry of cassiterite and its inclusions and exsolution products from tin and tungsten deposits in Portugal. *Can. Mineral.* **34**, 745-768.
- NOVÁK, M. & POVONDRA, P. (1995): Elbaite pegmatites in the Moldanubicum: a new subtype of the rare-element class. *Mineral. Petrol.* **55**, 159-176.
- PAULING, L. (1960): *The Nature of the Chemical Bond* (3rd ed.). Cornell Univ. Press, Ithaca, N.Y.
- POUCHOU, J.-L. & PICOIR, F. (1984): A new model for quantitative analysis. I. Application to the analysis of homogeneous samples. *La Recherche Aérospatiale* **3**, 13-38.
- \_\_\_\_\_, \_\_\_\_\_ (1985): "PAP" (phi-rho-Z) procedure for improved quantitative microanalysis. In *Microbeam Analysis* (J.T. Armstrong, ed.). San Francisco Press, San Francisco, California, (104-106).
- RUCK, R., DUSAUSOY, Y., NGUYEN TRUNG, C., GAITE, J.-M. & MURCIEGO, A. (1989): Powder EPR study of natural cassiterites and synthetic SnO<sub>2</sub> doped with Fe, Ti, Na and Nb. *Eur. J. Mineral.* **1**, 343-352.
- RUDAKOVA, Z.N. (1972): On the quantitative relationships of some elements in the composition of cassiterite. *Zap. Vses. Mineral. Obshchest.* **101**, 317-322 (in Russ.).
- SHANNON, R.D. (1976): Revised effective ionic radii and systematic studies of interatomic distances in halides and chalcogenides. *Acta Crystallogr.* **A32**, 751-767.

*Received September 2, 1999, revised manuscript accepted March 9, 2000.*